International Journal of Mechanics of Solids

E-ISSN: 2707-8078
P-ISSN: 2707-806X
Journal's Website
IJMS 2026; 7(1): 73-77
Received: xx-10-2025
Accepted: xx-11-2025

Manjula Ramagiri
Department of Mathematics
University Arts and Science College (Autonomous)
Kakatiya University
Warangal, Telangana, India

Corresponding Author:
Manjula Ramagiri
Department of Mathematics
University Arts and Science College (Autonomous)
Kakatiya University
Warangal, Telangana, India

The influence of initial stress on magnetic field-induced deformations in poroelastic hollow cylinders

Manjula Ramagiri

DOI: https://www.doi.org/10.22271/2707806X.2026.v7.i1b.62

Abstract
This work examines torsional wave propagation in a poroelastic hollow cylinder under the influence of a magnetic field and starting load. The frequency equation is derived using boundary conditions. The governing equations are formulated based on Biot's theory of deformation. The non-dimensional frequency is determined in relation to the ratio for various values of magnetic field and beginning stress. The theoretically generated results are calculated for two types of materials and displayed graphically.

Keywords: Poroelasticity, magnetic field, frequency equation, frequency, hollow cylinder, torsional vibrations, initial stress

1. Introduction

Wave propagation in poroelastic hollow cylinders has become very important in recent decades. The investigation of starting stress in a poroelastic hollow cylinder under magnetic field effects entails examining how initial stresses, poroelastic material characteristics, and external magnetic fields interact to affect the cylinder's mechanical, magnetic, and fluid flow properties. This is applicable in disciplines such as geophysics, biomedical engineering, and structural mechanics. The analysis of wave propagation in cylinders aimed to determine the frequencies associated with several modes of vibration: flexural, torsional, and longitudinal, through the formulation of a frequency equation. Initial stresses markedly modify the stiffness of the cylinder, affecting the natural frequencies and mode shapes of torsional vibrations. Elevated initial stress levels can either support or destabilize the cylinder, contingent upon their distribution and interaction with other forces. Comprehending how torsional vibrations react to magnetic fields and starting strains facilitates enhanced diagnostics in pipelines, boreholes, and biological applications. Resolving the coupled equations for torsional vibrations in poroelastic material influenced by magnetic fields is computationally demanding, necessitating sophisticated numerical techniques. The study examines magnetoelastic torsional waves in a bar subjected to initial load, as detailed in [1]. The investigation of torsional waves in a viscoelastic, initially strained cylinder situated within a magnetic field is presented in [2]. The torsional vibrations of a stiff circular plate on transversely isotropic saturated soil are examined in [3]. A transient torsional wave in a finite hollow cylinder with initial axial stress is discussed in [4]. The torsional vibrations of a non-homogeneous magnetostrictive elastic circular cylinder are examined in [5]. The study examines torsional waves in a pre-stressed fiber-reinforced media under the influence of a magnetic field, as detailed in [6]. The discussion in [7] pertains to magneto-electro-viscoelastic torsional waves in an aeolotropic tube subjected to initial compressive stress. The presence of torsional surface waves in a porous crustal layer situated above an initially stressed inhomogeneous half-space is discussed in [8]. The propagation of torsional surface waves in an inhomogeneous anisotropic fluid-saturated porous layered half-space under initial load with variable characteristics is examined in [9]. The impact of irregularities on torsional surface waves in an initially strained anisotropic porous layer situated between homogeneous and non-homogeneous half-spaces is examined in [10]. The impact of a corrugated boundary surface and a reinforced layer on the propagation of torsional surface waves is examined in [11]. The dispersion of torsional surface waves in an intermediate vertical pre-stressed inhomogeneous layer situated between heterogeneous half-spaces is discussed in [12].

The impact of initial conditions and gravity on torsional surface waves in heterogeneous media is discussed in [13]. The effects of longitudinal magnetic fields on the torsional vibrations of carbon nanotubes are examined in [14]. The investigation of torsional vibrations in a poroelastic dissipative thick-walled hollow cylinder under initial stress is presented in [15]. The study in [16] examines the torsional vibrations of irregular single-walled carbon nanotubes, considering the consequences of compressive starting stress. The study of torsional wave propagation in a sandwiched magneto-poroelastic dissipative transversely isotropic medium is discussed in [17]. The study of torsional waves in a dissipative cylindrical shell subjected to initial tension is presented in [18]. The study of torsional wave propagation in a porothermoelastic hollow cylinder is conducted in [19]. The study of torsional vibrations in magnetic field poroelastic hollow cylinders is examined in [20]. The study of initial stress effects on torsional vibrations in anisotropic magneto-poroelastic hollow cylinders is detailed in [21]. This research examines the influence of magnetic field and starting stress on torsional vibrations in a poroelastic hollow cylinder. The displacement components have been acquired. Upon applying appropriate boundary conditions, the frequency equation is derived in the context of a magnetic field and initial stress. The non-dimensional frequency is determined in relation to the ratio for various values of magnetic field and beginning stress. The results are ultimately presented in graphical format.

2. Governing equations and solution of the problem

Let $(\mathrm{r},\theta,\mathrm{z})$ be the cylindrical polar coordinates. Consider a homogenous isotropic hollow poroelastic cylinder with inner and outer radii a and b, respectively, whose axis is in the direction of z -axis. The equations of motion are given in [1]:

$$\frac{\partial\sigma_{rr}}{\partial r}+\frac{1}{r}\frac{\partial\sigma_{r\theta}}{\partial\theta}+\frac{\partial\sigma_{rz}}{\partial z}+\frac{\sigma_{rr}-\sigma_{\theta\theta}}{r}-P\frac{\partial\omega_{\theta}}{\partial z}+F_r=\frac{\partial^2}{\partial t^2}(\rho_{11}u+\rho_{12}U),$$
$$\frac{\partial\sigma_{\theta r}}{\partial r}+\frac{1}{r}\frac{\partial\sigma_{\theta\theta}}{\partial\theta}+\frac{\partial\sigma_{\theta z}}{\partial z}+\frac{2\sigma_{r\theta}}{r}+P\frac{\partial\omega_{\theta}}{\partial z}+F_{\theta}=\frac{\partial^2}{\partial t^2}(\rho_{11}v+\rho_{12}V),$$
$$\frac{\partial\sigma_{zr}}{\partial r}+\frac{1}{r}\frac{\partial\sigma_{z\theta}}{\partial\theta}+\frac{\partial\sigma_{zz}}{\partial z}+\frac{\sigma_{rz}}{r}-P(\frac{\partial\omega_{\theta}}{\partial r}-\frac{\partial\omega_{r}}{\partial\theta})+F_z=\frac{\partial^2}{\partial t^2}(\rho_{11}w+\rho_{12}W),$$

$$\frac{\partial s}{\partial r}=\frac{\partial^2}{\partial t^2}(\rho_{12}u+\rho_{22}U),$$

$$\frac{1}{r}\frac{\partial s}{\partial\theta}=\frac{\partial^2}{\partial t^2}(\rho_{12}v+\rho_{22}V),$$

$$\frac{\partial s}{\partial z}=\frac{\partial^2}{\partial t^2}(\rho_{12}w+\rho_{22}W). \tag{1}$$

Where $\vec{u}(u,v,w)$ and $\vec{U}(U,V,W)$ be the solid and fluid displacements. ρ_{ij} are mass coefficients. $\sigma_{rr},\sigma_{\theta\theta},\sigma_{zz},\sigma_{rz},\sigma_{r\theta},\sigma_{\theta z}$ are stresses components and ω_r,ω_{θ} are rotational components, fluid pressure s. $F=(F_r,F_{\theta},F_z)$ is the Lorentz force per unit volume due to the axial magnetic field is given by [1]

$$F=J\times B,\quad \omega_r=\frac{1}{2}(\frac{\partial w}{\partial\theta}-\frac{\partial v}{\partial\theta}),\quad \omega_r=\frac{1}{2}(\frac{\partial u}{\partial z}-\frac{\partial w}{\partial r}) \tag{2}$$

The stress components σ_{ij} and fluid pressure [22] are

$$\sigma_{ij}=2Ne_{ij}+(Ae+Q\varepsilon)\delta_{ij}\qquad (i,j=r,\theta,z),$$
$$s=Qe+R\varepsilon. \tag{3}$$

In eq. (3), e_{ij} 's strain displacements, σ_{ij} 's solid stresses and fluid pressure s, δ_{ij} the well-known Kroneckar delta function. e and ε are the dilatations of solid and fluid respectively; the symbols $\mathrm{A, N, Q, R}$ are all poroelastic constants. Maxwell equations governing the electromagnetic fields for slowly moving solid medium having electrical conductivity are [1]

$$curlH=4\pi J,\quad curlE=\frac{-1}{c}\frac{\partial B}{\partial t},\quad divB=0,\quad B=\mu_e H \tag{4}$$

Where displacement current is neglected and by ohm's law

$$J=\sigma(E+\frac{1}{c}\frac{\partial u}{\partial t}\times B) \tag{5}$$

In eq. (4) and (5) H,B,E,J are respectively the magnetic intensity, magnetic induction, electric intensity and current density vectors; μ_e,σ,u are magnetic permeability and electrical conductivity of the body, displacement vector in strained state and c is the velocity of light. The electromagnetic field equations in vacuum are [1]

$$(\nabla^2-\frac{1}{c^2}\frac{\partial^2}{\partial t^2})E^*=0,(\nabla^2-\frac{1}{c^2}\frac{\partial^2}{\partial t^2})h^*=0,$$
$$CurlE^*=-\frac{1}{c}\frac{\partial h^*}{\partial t},Curlh^*=\frac{1}{c}\frac{\partial E^*}{\partial t}. \tag{6}$$

Where h^* the perturbation is magnetic field in vacuum and E^* is the electric field in vacuum. Now let suppose that $H=H_0+h$, where H_0 the initial magnetic field acting parallel to is h is small perturbation in the field. If the cylinder is a perfect conductor of electricity (i.e, $\sigma\to\infty$) hence eq. (5) gives

$$E=\frac{-1}{c}\frac{\partial u}{\partial t}\times B=(\frac{-H}{c}\frac{\partial v}{\partial t},0,0) \tag{7}$$

Where $H=|H_0|$. Eliminating E from eq. (4) and eq. (7) we obtain

$$h=(0,H\frac{\partial v}{\partial z},0) \tag{8}$$

From eq. (4) and eq. (8) we get

$$J \times B = J \times \mu_e H = (0, \frac{-H^2}{4\pi}\frac{\partial^2 v}{\partial z^2}, 0) \quad (9)$$

In the case of torsional vibrations, the equations of motion eq. (1) reduced to the following equations:

$$\frac{\partial \sigma_{\theta r}}{\partial r} + \frac{\partial \sigma_{\theta z}}{\partial z} + \frac{2\sigma_{r\theta}}{r} - (\frac{P}{2} - \frac{H^2}{4\pi})\frac{\partial^2 v}{\partial z^2} = \frac{\partial^2}{\partial t^2}(\rho_{11} v + \rho_{12} V), \quad (10)$$
$$0 = \frac{\partial^2}{\partial t^2}(\rho_{12} v + \rho_{22} V).$$

Assume that the wave solution takes the following form

$$v(r) = v_1(r) e^{ik(z-\omega t)}, \quad V(r) = V_1(r) e^{ik(z-\omega t)}. \quad (11)$$

In eq. (11) ω is the frequency, k is the wavenumber, and t is time. Substituting eq. (11) and eq. (3) in eq. (10), we obtains

$$N\frac{d^2 v_1}{dr^2} + \frac{N}{r}\frac{dv_1}{dr} - N\frac{v_1}{r^2} - k^2 N(\frac{P}{2} - \frac{H^2}{4\pi})v_1 = -\omega^2(\rho_{11} v_1 + \rho_{12} V_1), \quad (12)$$
$$0 = -\omega^2(\rho_{12} v_1 + \rho_{22} V_1)$$

The solution of eq. (12) takes the following form

$$v_1(r) = [AJ_1(qr) + BY_1(qr)]e^{ik(z-\omega t)}, \quad V_1(r) = \frac{-\rho_{11}}{\rho_{22}}[AJ_1(qr) + BY_1(qr)]e^{ik(z-\omega t)}. \quad (13)$$

Where $q = \frac{\omega^2}{V_s^2} - k^2(\frac{P}{2} - \frac{H^2}{4\pi N})$. A, B are the arbitrary constants and $J_1(qr), Y_1(qr)$ are Bessel's functions of first kind. V_s is the shear wave velocity [7]. The non-zero stresses are

$$\sigma_{r\theta} = A[NqJ_0(qr) - \frac{2N}{r}J_1(qr)] + B[NqY_0(qr) - \frac{2N}{r}Y_1(qr)]. \quad (14)$$

3. Boundary conditions and frequency equation

The boundary conditions that define the inner and outer surfaces are unconstrained at

$r = a$ and $r = b$ are
$\sigma_{r\theta} = 0$ at $r = a$ and
$\sigma_{r\theta} = 0$ at $r = b$ (15)

By employing equations (15) and (14), we get two homogeneous equations.

$$A[NpJ_0(qa) - \frac{2N}{a}J_1(qa)] + B[NpY_0(qa) - \frac{2N}{a}Y_1(qa)] = 0,$$
$$A[NpJ_0(qb) - \frac{2N}{b}J_1(qb)] + B[NpY_0(qb) - \frac{2N}{b}Y_1(qb)] = 0. \quad (16)$$

By eliminating the constants, we derive the frequency equation.

$$\begin{vmatrix} A_{11} & A_{12} \\ A_{21} & A_{22} \end{vmatrix} = 0 \quad (17)$$

4. Non-dimensional for the frequency equation

To find the frequency equation it is necessary to introduce non-dimensional quantities

$$a_4 = \frac{N}{H_1}, d_1 = \frac{\rho_{11}}{\rho}, \quad d_2 = \frac{\rho_{12}}{\rho}, \quad d_3 = \frac{\rho_{22}}{\rho},$$
$$\tilde{z} = \left(\frac{V_0}{V_3}\right)^2, \quad m = \frac{c}{c_0}, \; c = \frac{\omega}{k}, \Omega = \frac{\omega h}{c_0} \quad (18)$$

In the eq (18), c is the phase velocity, c_0 and V_0 are reference velocities $(c_0^2 = N\rho^{-1}, V_0^2 = H_1\rho^{-1})$ and then m is non-dimensional phase velocity, Ω is non-dimensional frequency and $\rho = \rho_{11} + 2\rho_{12} + \rho_{22}$, $H_1 = P + 2Q + R$.

5. Numerical results

The numerical results consider two types of materials: cylinder-I, composed of water-saturated sandstone, and cylinder-II, composed of kerosene-saturated sandstone, as referenced in [23, 24]. The non-dimensional parameters are presented in Table I.

Table 1: The non-dimensional parameters are presented

Materials	a_4	d_1	d_2	d_3	Z
Cylinder-I	0.412	0.877	0	0.123	2.129
Cylinder-II	0.234	0.901	-0.001	0.101	3.851

For specified poroelastic materials, the derived frequency equation, when non-dimensionalized using equation (18), establishes a relationship between the non-dimensional frequency and the ratio. The non-dimensional frequency is calculated for both cylinder-I and cylinder-II. The non-dimensional frequency is calculated for various values of the ratio, initial stress, and magnetic field. Figure 1 illustrates the non-dimensional frequency plotted against the ratio for cylinder-I. The non-dimensional frequency reaches its peak at h=0.6 as the initial stress and magnetic field increase, exhibiting periodic characteristics. Figure 2 illustrates the non-dimensional frequency plotted against the ratio for cylinder-II. The non-dimensional frequency reaches its maximum at h=0.4 as the initial stress and magnetic field increase. Figure 3 illustrates the non-dimensional frequency plotted against the ratio for cylinder-I and cylinder-II. All the figures clearly indicate that the curves are periodic in character. Typically, the values of cylinder-II exceed those of cylinder-I. The data clearly indicate that the values for cylinder II exceed those of cylinder I. The effects arise from magnetic coupling and initial stress within the solid component.

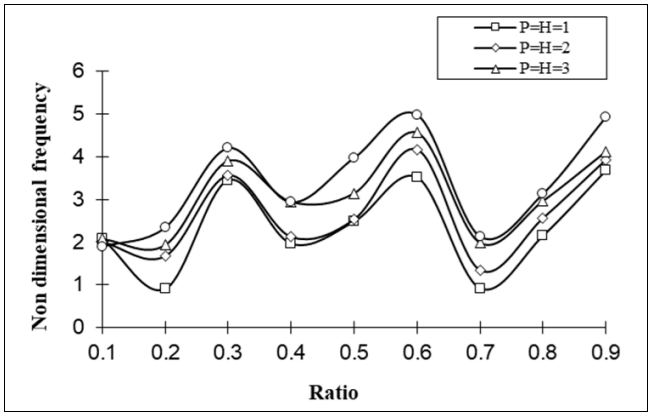

Fig 1: Nondimensional frequency versus ratio for different initial stress and magnetic field for cylinder-I

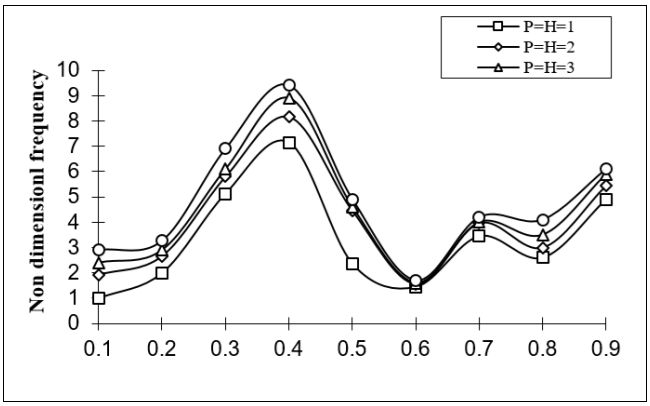

Fig 2: Nondimensional frequency versus ratio for different initial stress and magnetic field for cylinder-II

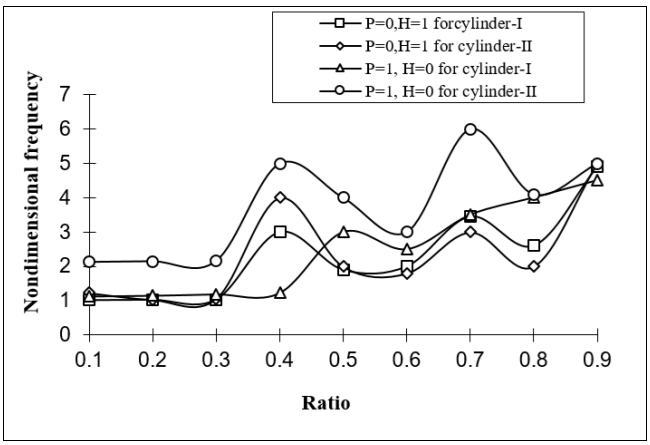

Fig 3: Nondimensional frequency versus ratio for different initial stress and magnetic field

Conclusion

The torsional vibrations of a poroelastic hollow cylinder subjected to a magnetic field and initial stress stress have been investigated. The research highlights the significance of evaluating the synergistic effects of initial stress magnetic fields and poroelasticity in the analysis of torsional vibrations in hollow cylinders. These discoveries possess extensive applications in engineering, geophysics, biomechanics, and materials science, facilitating the development of more resilient and efficient designs in difficult environmental situations. The frequency equation is derived considering the influence of the magnetic field and initial stress. In all instances, as the ratio grows, the frequency exhibits periodic characteristics.

References

1. Naraian. Magnetoelastic torsional waves in a bar under initial stress. Proceedings of the Indian Academy of Sciences Section A. 1978;87(5):137–145.
2. Naraian S. Torsional waves in a viscoelastic initially stressed cylinder placed in a magnetic field. Proceedings of the National Academy of Sciences India Section A. 1984;54(3):10–20.
3. Wu D, Cai Y, Xu C, Zhang H. Torsional vibrations of rigid circular plate on transversely isotropic saturated soil. Applied Mathematics and Mechanics. 2006;27(11):1541–1548.
4. Wang H, Chen W. Transient torsional wave in finite hollow cylinder with initial axial stress. Acta Mechanica Solida Sinica. 2008;21(6):536–541.
5. Abd Alla AM, Debnath L. Torsional vibrations of non-homogeneous magnetostrictive elastic circular cylinder. International Journal of Mathematics and Mathematical Sciences. 1994;17(1):181–186.
6. Kakar R, Kakar S. Torsional waves in prestressed fiber reinforced medium subjected to magnetic field. Journal of Solid Mechanics. 2012;4(4):402–415.
7. Kakar R. Magneto-electro-viscoelastic torsional waves in aeolotropic tube under initial compression stress. Latin American Journal of Solids and Structures. 2014;11:580–597.
8. Gupta S, Sultana R, Verma AK. Existence of torsional surface waves in porous crustal layer over an initially stressed inhomogeneous half space. Journal of Vibration and Control. 2014;22(7):1717–1728.
9. Shekar S, Parvez I. Propagation of torsional surface waves in an inhomogeneous anisotropic fluid-saturated porous layered half space under initial stress with varying properties. Applied Mathematical Modelling. 2016;40(2):1300–1314.
10. Kundu A, Gupta S, Vaishnav PK. Effects of irregularity on torsional surface waves in an initially stressed anisotropic porous layer sandwiched between homogeneous and non-homogeneous half space. Journal of Earth System Science. 2016;125(4):885–895.
11. Singh AK, Lakshman A, Chattopadhyay A. Influence of corrugated boundary surface and reinforced layer on propagation of torsional surface wave. Journal of Vibration and Control. 2016;23(9):1417–1436.
12. Kakar R, Kakar S. Dispersion of torsional surface wave in an intermediate vertical prestressed inhomogeneous layer lying between heterogeneous half space. Journal of Vibration and Control. 2016;23(19):3292–3369.

13. Mukhopadhyay, Gupta AK, Kundu S. Influence of initial stress and gravity on torsional surface wave in heterogeneous medium. Journal of Vibration and Control. 2017;23(6):970–979.
14. Arda M, Aydogdu M. Longitudinal magnetic field effects on torsional vibrations of carbon nanotubes. Journal of Computational and Applied Mechanics. 2018;49(2):304–313.
15. Balu C, Modem R, Bandari SR, Reddy PM. Study of torsional vibrations in poroelastic dissipative thick-walled hollow cylinder in the presence of initial stress. Special Topics and Reviews in Porous Media – An International Journal. 2019;10(5):447–456.
16. Selim M. Torsional vibrations of irregular single-walled carbon nanotubes incorporating compressive initial stress effects. Journal of Mechanics. 2021;37(5):260–269.
17. Radhika B, Balu C, Reddy PM, Rao S. Investigation of torsional wave propagation in sandwiched magnetoporoelastic dissipative transversely isotropic medium. Advances and Applications in Mathematical Sciences. 2021;20(9):2393–2418.
18. Selim M, Khaled, GePreet. Torsional wave in a dissipative cylindrical shell under initial stress. Computers, Materials and Continua. 2022;70(2):3021–3030.
19. Ramagiri M. Torsional wave propagation in a porothermoelastic hollow cylinder. International Journal for Modern Trends in Science and Technology. 2019;5(6):27–30.
20. Ramagiri M. Investigation of torsional vibrations in magnetic field poroelastic hollow cylinders. Caribbean Journal of Science and Technology. 2022;10(1):36–42.
21. Ramagiri M, Sree Lakshmi T, Chandulal A. Investigation of initial stress on torsional vibrations in anisotropic magneto-poroelastic hollow cylinders. Ponte: International Journal of Sciences and Research. 2023;79(1):24–30.
22. Biot MA. Theory of propagation of elastic waves in a fluid-saturated porous solid. Journal of the Acoustical Society of America. 1956;28:168–178.
23. Yew CH, Jogi PN. Study of wave motions in fluid-saturated porous rocks. Journal of the Acoustical Society of America. 1976;60:2–8.
24. Fatt I. The Biot–Willis elastic coefficient for a sandstone. Journal of Applied Mechanics. 1956;23:296–297.